Conformational Properties of 2,4-Methanoproline (2-Carboxy-2,4-methanopyrrolidine) in Peptides: Determination of Preferred Peptide Bond Conformation in Aqueous Solution by Proton Overhauser Measurements

Gaetano T. Montelione, Philip Hughes, Jon Clardy, and Harold A. Scheraga*

Contribution from the Baker Laboratory of Chemistry, Cornell University, Ithaca, New York 14853-1301. *Received October 15, 1985*

Abstract: The effects of replacing L-proline with a novel naturally occurring α-amino acid, 2,4-methanoproline (2-carboxy-2,4-methanopyrrolidine; 2,4-MePro), on the tertiary peptide bond cis/trans equilibrium have been investigated in small peptides by nuclear magnetic resonance spectroscopy. In aqueous solution, both Ac-2,4-MePro-NHMe and Ac-L-Tyr-2,4-MePro-NHMe are found to adopt primarily (≥95%) a single X-2,4-MePro peptide bond conformation, while the corresponding L-proline peptides exist as an equilibrium mixture of approximately isoenergetic cis and trans conformers. ^{1}H NMR resonance assignments for these 2,4-MePro-containing peptides are obtained by double quantum filtered homonuclear correlated spectroscopy. The known interproton distances within the 2,4-methanoproline side chain are used to calibrate data from truncated Overhauser effect measurements. With this calibration, data from interresidue nuclear Overhauser effect measurements are used together with distance geometry considerations to demonstrate that the preferred conformation of the X-2,4-MePro peptide bond in both Ac-2,4-MePro-NHMe and Ac-Tyr-2,4-MePro-NHMe is trans in aqueous solution. This conclusion was confirmed by similar qualitative evaluation of the two-dimensional nuclear Overhauser effect (NOESY) spectrum. These results suggest that 2,4-MePro may be a useful L-proline analogue for polypeptide molecular design, since the trans peptide bond conformation is selectively stabilized.

It is generally recognized that, while the planar peptide groups of secondary amino acid amides adopt predominantly the trans C^α/C^α conformation, those of tertiary amides (e.g., X-Pro groups) have approximately the same energy in both the cis and trans forms.[1-6] This trans/cis conformational heterogeneity can confer important biological and pharmacological properties on proteins and peptides. For example, the rate-limiting step in the refolding of proteins from disordered conformational distributions with nonnative X-Pro peptide bond conformations may often correspond to trans/cis proline isomerization.[7-10] X-Pro peptide bond isomerization may also give rise to a kinetic barrier between multiple functionally distinct native conformations of polypeptides and proteins, as has been suggested for concanavalin A[11] and bovine prothrombin.[12] From these findings, it is clear that proline analogues for which the trans or cis peptide bond conformation is selectively stabilized will be useful tools for investigating the roles of proline isomerization in biochemical processes and in the design of polypeptide drugs.

Recently, several reports[13-16] have appeared describing the conformational properties of proline analogues in peptides. From these studies, two proline analogues, 5-oxo-L-proline[13] and 2-methylproline,[14-16] for which the trans peptide bond conformation is preferentially stabilized (>98%) in aqueous solution, have been identified. Unfortunately, incorporation of 5-oxo-L-proline into a polypeptide results in the formation of an imide functional group, which is highly susceptible to base-catalyzed hydrolysis in aqueous solution.[13] 5-Oxo-L-proline is therefore an unacceptable proline analogue for polypeptide molecular design. Peptides containing 2-methylproline, on the other hand, are quite stable in aqueous solution.

Motivated by these studies, we are examining the conformational properties of a related proline analogue, 2,4-methanoproline.[17-19] This paper is the first report of the conformational properties of 2,4-methanoproline in peptides. The crystal structure of this novel, naturally occurring α-amino acid, which contains no chiral atoms, has been reported elsewhere.[17] A model of the amino acid with terminal blocking groups and all trans peptide bonds [i.e., *trans*-Ac-2,4-MePro-NHMe], along with the nomenclature that we have adopted for the 2,4-methanopyrrolidine side chain, is presented in Figure 1. In this paper, we describe

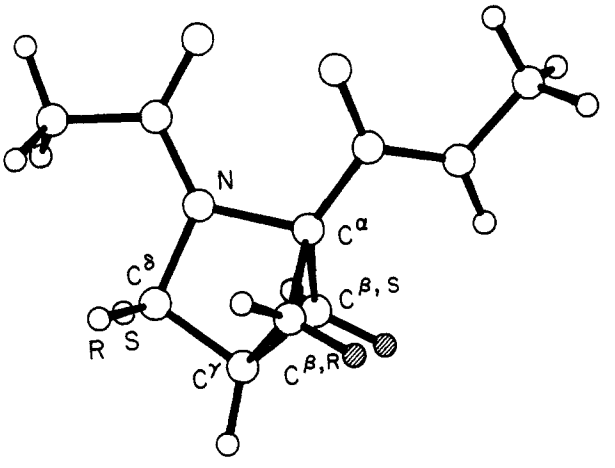

Figure 1. *trans*-Ac-2,4-MePro-NHMe. In the notation used here, R and S designate *pro-R* and *pro-S* prochirality assignments of the C^β atoms with respect to the C^α carbon atom and of the $C^\delta H$ protons with respect to the C^δ carbon atom. The exo $C^\beta H$ hydrogen atoms are shaded. In the notation used for describing conformations of polypeptide chains, $C^{\beta,R}$ is denoted $C^{\beta,1}$ and $C^{\beta,S}$ is denoted $C^{\beta,2}$.

^{1}H NMR studies which, combined with distance geometry considerations, were used to determine that replacement of L-proline

* To whom requests for reprints should be addressed.

(1) Madison, V.; Schellman, J. *Biopolymers* **1970**, *9*, 511.
(2) Stewart, W. E.; Siddall, T. H. *Chem. Rev.* **1970**, *70*, 517.
(3) Thomas, W. A.; Williams, M. K. *J. Chem. Soc., Chem. Commun.* **1972**, 994.
(4) Grathwohl, C.; Wüthrich, K. *Biopolymers* **1976**, *15*, 2025.
(5) Grathwohl, C.; Wüthrich, K. *Biopolymers* **1976**, *15*, 2043.
(6) Zimmerman, S. S.; Scheraga, H. A. *Macromolecules* **1976**, *9*, 408.
(7) Brandts, J. F.; Halvorson, H. R.; Brennan, M. *Biochemistry* **1975**, *14*, 4953.
(8) Lin, L.-N.; Brandts, J. F. *Biochemistry* **1978**, *17*, 4102.
(9) Lin, L.-N.; Brandts, J. F. *Biochemistry* **1983**, *22*, 559.
(10) Lin, L.-N.; Brandts, J. F. *Biochemistry* **1983**, *22*, 573.
(11) Brown, R. D.; Brewer, C. F.; Koenig, S. H. *Biochemistry* **1977**, *16*, 3883.
(12) Marsh, H. C.; Scott, M. E.; Hiskey, R. G.; Koehler, K. A. *Biochem. J.* **1979**, *183*, 513.
(13) Galardy, R. E.; Alger, J. R.; Liakopoulou-Kyriakides, M. *Int. J. Pept. Protein Res.* **1982**, *19*, 123.

0002-7863/86/1508-6765$01.50/0

with 2,4-methanoproline in either Ac-L-Pro-NHMe or Ac-L-Tyr-L-Pro-NHMe conformationally restricts the X-Pro peptide bond exclusively (≳95%) to the trans conformation in aqueous solution.

Methods

Peptide Synthesis. All peptides used in this study were analyzed by high-performance liquid chromatography (HPLC) on a Spectra Physics SP8000 liquid chromatography system using a reversed phase C_{18} column and 214-nm ultraviolet absorbance detection. Synthetic intermediates and products were characterized by ^1H and ^{13}C NMR spectroscopy.

The photochemical synthesis and characterization of the α-amino acid 2,4-methanoproline have been described elsewhere.[18] Both Ac-2,4-MePro-NHMe and Ac-L-Tyr-2,4-MePro-NHMe were synthesized from the benzyl ester of 2,4-methanoproline by classical peptide synthetic methods. This benzyl ester starting material was prepared as a tosylate salt (2,4-MePro-OBz·TsO⁻) by refluxing 2,4-methanoproline (900 mg) and toluenesulfonic acid (1.1 molar equivalents) in benzene (12 mL) and benzyl alcohol (8 mL) for 16 h with azeotropic removal of water. The cooled reaction mixture was poured into ether to precipitate the product (2,4-MePro-OBzl·TsO⁻) (2.4 g) which was collected in essentially quantitative yield.

Ac-2,4-MePro-NHMe was prepared according to the following procedure. First, (2,4-MePro-OBzl·TsO⁻) (500 mg) was dissolved in methylene chloride (5 mL) containing triethylamine (2.5 molar equiv) and treated with acetyl chloride (1.1 molar equiv). The solvent was then removed in vacuo and the residue, containing Ac-2,4-MePro-OBzl, was dissolved in 40% aqueous methylamine (10 mL), sealed, and heated on a steam bath for 3 h. Following removal of the solvent in vacuo, the product, Ac-2,4-MePro-NHMe, was purified by silica gel chromatography (9:1, CH_2Cl_2:MeOH) and subsequently recrystallized several times from ethyl acetate. The structure was confirmed by ^1H and ^{13}C NMR spectroscopy. The crystalline compound exhibited a single (>99.5%) symmetric peak on reverse-phase HPLC with use of a linear gradient of acetonitrile in 0.09% TFA (2% to 25% acetonitrile over 40 min); mp 133–135 °C; R_f 0.7 (9:1, CH_2Cl_2:MeOH).

Ac-L-Tyr-2,4-MePro-NHMe was also synthesized from (2,4-MePro-OBzl·TsO⁻), according to the following procedure. A solution of (2,4-MePro-OBzl·TsO⁻) (1 g) in 40% aqueous methylamine (15 mL) was sealed and heated on a steam bath for 3 h. The mixture was concentrated in vacuo and applied to a weak cation exchange column (1.5 × 10 cm, CGC-270, Ionac Chemical Co., H^+ form) previously equilibrated with distilled water. The product, 2,4-MePro-NHMe, was eluted with 0.5 N NH_4OH. The solvent was removed in vacuo to yield 340 mg (96%) of 2,4-MePro-NHMe.

In the next step of the synthesis, 2,4-MePro-NHMe was coupled to Boc-L-Tyr to form Boc-L-Tyr-2,4-MePro-NHMe. 2,4-MePro-NHMe (340 mg) and Boc-L-Tyr (1.1 molar equiv, Sigma Chemical Co.) were dissolved in dimethylformamide (3.5 mL) and treated with *N,N'*-dicyclohexylcarbodiimide (DCC, 1.1 molar equiv). The mixture was stirred at room temperature for 3 h and then diluted with acetonitrile (20 mL) and filtered through Celite. The filtrate was concentrated and dried in vacuo. The product, Boc-L-Tyr-2,4-MePro-NHMe (688 mg, 70%), was isolated following chromatography on silica gel (9:1 CH_2Cl_2:MeOH).

In the final stage of the synthesis, Boc-L-Tyr-2,4-MePro-NHMe was deprotected and acylated. Boc-L-Tyr-2,4-MePro-NHMe (688 mg) was dissolved in 30% (v/v) trifluoroacetic acid in methylene chloride (6.5 mL total) and stirred for 3 h at room temperature. The reaction mixture was then concentrated and dried in vacuo to give the deprotected dipeptide, L-Tyr-2,4-MePro-NHMe. This material was then N-acylated by dissolving the residue in ethanol (3 mL) containing triethylamine (2.2 molar equiv) and treating the mixture with 4-nitrophenylacetate followed by stirring for 16 h. The solvent was then removed in vacuo and the product, Ac-L-Tyr-2,4-MePro-NHMe (493 mg, 84%), isolated following chromatography on silica gel (9:1 CH_2Cl_2:MeOH). The solvent was removed in vacuo, and the dipeptide was recrystallized from ethyl acetate at 4 °C. The structure was confirmed by ^1H and ^{13}C NMR spectroscopy. The crystalline peptide exhibited a single (>99%) symmetric peak on reverse-phase HPLC using a linear gradient of acetonitrile in 0.09% TFA (2 to 25% acetonitrile over 40 min); mp 187–190 °C dec; R_f 0.31 (95:20:3 $CHCl_3$:MeOH:AcOH).

NMR Instrumentation and Sample Preparation. ^1H NMR spectra were obtained at 300 MHz with a Bruker WM-300 spectrometer equipped with an Aspect 2000A computer. The probe temperature was thermostated at 25 ± 1 °C. For conventional one-dimensional ^1H NMR spectroscopy, a spin-recovery delay was inserted between pulses (resulting in a total spin-recovery time greater than 5 s) to avoid relaxation modulation of relative resonance intensities. ^{13}C NMR spectra were recorded in 8 mm diameter NMR tubes at 22.5 MHz and room temperature with a JEOL FX92Q spectrometer. ^1H and ^{13}C NMR samples were prepared at a concentration of 5–10 mg/mL in deuterium oxide-d_2 (99.96% D, Stohler Isotopes) at pH* 6 to 7 (pH* being the pH meter reading of D_2O solution) or in dimethyl-d_6 sulfoxide (100.0% D, Stohler Isotopes). No dependence of the spectroscopic measurements on peptide concentration was observed. Chemical shifts in D_2O are reported relative to δ_{HOD} = 4.78 ppm.

Steady State Truncated Driven Proton Overhauser Effect Measurements. Difference proton Overhauser effect measurements were obtained by the method of Wagner and Wuthrich.[20] The data were multiplied by a simple exponential smoothing function, corresponding to 0.5 Hz of line broadening. The relative NOEs reported (η) are the ratios of the integrated areas of resonances exhibiting an NOE to the area of the selectively irradiated resonance. When the resonances exhibiting an NOE arise from more than one equivalent proton, the value of η reported is the observed ratio divided by this number of equivalent protons.

NOE buildup curves were generated from sets of NOE difference spectra in which the length of the selective irradiation pulse was varied between 0.05 and 10 s. The values of the steady state NOEs reported in the Results Section are the plateau values obtained from the buildup curves. Cross-relaxation rates, estimated from the initial slopes[20] of the buildup curves, were used in calculating the optimum mixing times for NOESY spectra.

Two-Dimensional ^1H NMR Spectroscopy. Double quantum filtered proton correlated spectroscopy (DQF-COSY) was carried out as described elsewhere.[21-23] Phase-sensitive quadrature detection in ω1 was obtained by time-proportional phase incrementation.[24,25] Pure absorption mode NOE correlated spectroscopy (NOESY) was carried out as described elsewhere,[26-29] except that phase-sensitive quadrature detection in ω1 was obtained by time-proportional phase incrementation.[24,25] Optimum mixing times, τ_{mix}, were estimated by using data obtained from inversion-recovery measurements of longitudinal relaxation times and estimates of interproton cross-relaxation rates obtained from truncated driven NOE[20] buildup curves (described above). Cross-peaks arising from coherent magnetization transfer (J cross-peaks) were suppressed by appropriate phase cycling,[30] except those arising from zero-quantum coherence transfer which were suppressed by random variation of the mixing time[30] (τ_{mix}) by ≲33 ms, sufficient to suppress zero-quantum coherence between resonances separated by ≳15 Hz. Relative cross-peak areas were estimated from absorption-mode NOESY spectra by taking the average cross-peak to diagonal-peak integrated areas of several ω1 cross sections.

Calculations of Interproton Distances. Unless otherwise noted, the geometries of the amino acid residues used are those of the computer program ECEPP (Empirical Conformational Energy Program for Peptides).[31,32] The crystal structure of the terminally blocked amino acid *N*-acetyl-*N'*-methyl-2,4-methanoprolinamide (Ac-2,4-MePro-NHMe) will be reported elsewhere.[33] This crystal structure, with a crystallo-

(14) Delaney, N. G.; Madison, V. *Int. J. Pept. Protein Res.* **1982**, *19*, 543.
(15) Delaney, N. G.; Madison, V. *J. Am. Chem. Soc.* **1982**, *104*, 6635.
(16) Flippen-Anderson, J. L.; Gilardi, R.; Karle, I. L.; Frey, M. H.; Opella, S. J.; Gierasch, L. M.; Goodman, M.; Madison, V.; Delaney, N. G. *J. Am. Chem. Soc.* **1983**, *105*, 6609.
(17) Bell, E. A.; Qureshi, M. Y.; Pryce, R. J.; Janzen, D. H.; Lemke, P.; Clardy, J. *J. Am. Chem. Soc.* **1980**, *102*, 1409.
(18) Hughes, P.; Martin, M.; Clardy, J. *Tetrahedron Lett.* **1980**, *21*, 4579.
(19) Thoughout the text, we have adopted the abbreviations 2,4-MePro and mPro for the α-amino acid 2,4-methanoproline (2-carboxy-2,4-methanopyrrolidine) and Ac- and -NHMe for terminal acetyl and *N*-methyl groups, respectively.
(20) Wagner, G.; Wüthrich, K. *J. Magn. Reson.* **1979**, *33*, 675.
(21) Piantini, U.; Sørensen, O. W.; Ernst, R. R. *J. Am. Chem. Soc.* **1982**, *104*, 6800.
(22) Shaka, A. J.; Freeman, R. *J. Magn. Reson.* **1983**, *51*, 169.
(23) Rance, M.; Sørensen, O. W.; Bodenhausen, G.; Wagner, G.; Ernst, R. R.; Wüthrich, K. *Biochem. Biophys. Res. Commun.* **1983**, *117*, 479.
(24) Redfield, A. G.; Kunz, S. D. *J. Magn. Reson.* **1975**, *19*, 250.
(25) Marion, D.; Wüthrich, K. *Biochem. Biophys. Res. Commun.* **1983**, *113*, 967.
(26) Aue, W. P.; Bartholdi, E.; Ernst, R. R. *J. Chem. Phys.* **1976**, *64*, 2229.
(27) Jeener, J.; Meier, B. H.; Bachmann, P.; Ernst, R. R. *J. Chem. Phys.* **1979**, *71*, 4546.
(28) Macura, S.; Ernst, R. R. *Mol. Phys.* **1980**, *41*, 95.
(29) Wider, G.; Macura, S.; Kumar, A.; Ernst, R. R.; Wüthrich, K. *J. Magn. Reson.* **1984**, *56*, 207.
(30) Macura, S.; Huang, Y.; Suter, D.; Ernst, R. R. *J. Magn. Reson.* **1981**, *43*, 259.
(31) Momany, F. A.; McGuire, R. F.; Burgess, A. W.; Scheraga, H. A. *J. Phys. Chem.* **1975**, *79*, 2361.
(32) Némethy, G.; Pottle, M. S.; Scheraga, H. A. *J. Phys. Chem.* **1983**, *87*, 1883.

Table I. Geometry Used for Calculations of Interresidue Interproton Distances for X-2,4-MePro between the C^{α} Proton of Residue X and the $C^{\delta}H$ Protons of the Symmetrized 2,4-Methanopyrrolidine Side Chain

	trans	cis
bond lengths (Å)		
C^{α}–H (X)[a]	1.09[b]	1.09[b]
C^{α}–C′ (X)	1.53[c]	1.53[c]
C′–N (X–mPro)	1.34[d]	1.34[d]
N–C^{δ} (mPro)	1.49[d]	1.49[d]
C^{δ}–H (mPro)[e]	1.09[f]	1.09[f]
bond angles (deg)		
$HC^{\alpha}C'$ (X)	109.5[c]	109.5[c]
$C^{\alpha}C'N$ (X–mPro)	116[d]	116[d]
$C'NC^{\delta}$ (X–mPro)	128[d]	128[d]
$NC^{\delta}H$ (mPro)[e]	113[f]	113[f]
$H^{R}C^{\delta}H^{S}$ (mPro)	107[f]	107[f]
dihedral angles (deg)		
HC^{α}–C′N (X)	variable	variable
$C^{\alpha}C'$–NC^{δ} (X–mPro)	0	180
C′N–$C^{\delta}H^{R}$ (mPro)	−61[f]	61[f]
C′N–$C^{\delta}H^{S}$ (mPro)	61[f]	−61[f]

[a] The symbols in parentheses designate the moiety with which the corresponding bond length, bond angle, or dihedral angle is associated, viz., X, the L-α-amino acid preceding 2,4-methanoproline; mPro, the 2,4-methanoproline residue; X-mPro, the intervening peptide bond. [b] Corrected ECEPP[32] C^{α}–H bond length for L-α-amino acids in polypeptides. [c] Standard ECEPP[31] geometry for L-tyrosine. [d] Value obtained for symmetrized[34] crystal structure[33] of *trans*-Ac-2,4-MePro-NHMe. [e] These values are identical for the *pro-R* and *pro-S* $C^{\delta}H$ protons of 2,4-methanoproline. [f] Protons were added to the heavy atoms of the symmetrized[34] crystal structure[33] of *trans*-Ac-2,4-MePro-NHMe in idealized positions with use of standard methods.[35]

graphic residual $r = 0.05$, exhibits minor asymmetry of the methanopyrrolidine side chain which appears to arise from intramolecular strain imposed by the bicyclic ring structure. Because the magnitudes of interproton distances are affected only slightly by this side-chain asymmetry, and because precise data on the magnitude of the ensemble-averaged asymmetry in solution are not available, we assume a symmetric 2,4-methanopyrrolidine ring geometry in all of the calculations of interproton distances described in this paper.

For the calculations presented in this paper, the positions of the heavy atoms (C and N) of the terminally blocked amino acid crystal structure were symmetrized. The details of this symmetrization procedure will be described elsewhere.[34] Since hydrogens are not located accurately in electron density maps, they were added to the symmetric structure in idealized positions corresponding to a standard set of amino acid residue geometry[32,35] with 1.09 Å C–H bond lengths and 107° H–C–H bond angles. The resulting symmetrized 2,4-methanopyrrolidine side chain was used to calculate the intraresidue interproton distance matrix.

Conformation-dependent X $C^{\alpha}H$/2,4-MePro $C^{\delta}H$ interproton distances for X-2,4-MePro,[36] which (for fixed 2,4-methanopyrrolidine side-chain geometry) depends on the backbone dihedral angles ψ_X and ω_X, were calculated from standard vector-algebraic considerations, using methods similar to those described elsewhere.[37] The bond lengths, bond angles, and fixed dihedral angles for constructing the H–C^{α}–C′–N–C^{δ}–H fragments used in distance calculations for trans and cis X-2,4-MePro peptide bond (ω) conformations are listed in Table I.

Calculations of Vicinal Coupling Constants. Three-bond HC–C′H′ proton vicinal coupling constants were estimated for the symmetrized 2,4-methanoproline residue from the Karplus relationship[38,39]

$$^{3}J(\mathrm{HC\text{–}C'H'}) = 4.22 - 0.5\cos\theta + 4.5\cos 2\theta \qquad (1)$$

which is a theoretical result (in Hertz) of valence bond calculations for an *unstrained* HCC′H ethane fragment. The effects of bond angle and bond length distortions and of substituent electronegativity were not considered.

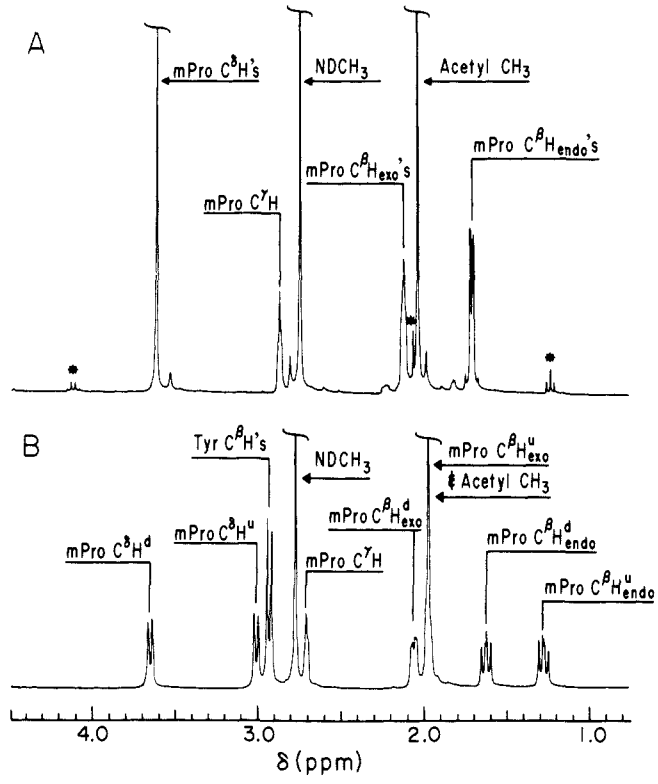

Figure 2. ^{1}H NMR spectra of (A) Ac-2,4-MePro-NHMe and (B) Ac-L-Tyr-2,4-MePro-NHMe in D_2O solution at 25 °C. In order to determine if the unlabeled minor resonances present in the A spectrum are due to a contaminating molecule, the peptide was recrystallized several times from ethyl acetate. The material used to obtain this spectrum (A) comes from a dissolved single crystal. Peaks marked with an asterisk correspond to small amounts of ethyl acetate associated with this crystal.

Results

X-2,4-MePro Peptide Bond Isomerization. ^{1}H NMR spectra of the aliphatic resonances of Ac-2,4-MePro-NHMe and Ac-L-Tyr-2,4-MePro-NHMe are presented in Figure 2, A and B, respectively. The assignments of proton resonances which are indicated in these figures were determined unambiguously from the DQF–COSY and NOESY data. Details about how these proton resonance assignments are made are described below. For Ac-2,4-MePro-NHMe, the two $C^{\beta}H^{exo}$, two $C^{\beta}H^{endo}$, and two $C^{\delta}H$ protons have degenerate resonance frequencies (Figure 2A), while in Ac-L-Tyr-2,4-MePro-NHMe the ensemble-averaged chemical shift anisotropy due to the aromatic tyrosine side chain breaks this degeneracy (Figure 2B). As a result of this "ring current shift", the pro-chiral $C^{\beta}H^{exo}$, $C^{\beta}H^{endo}$, and $C^{\delta}H$ proton pairs are resolved in the ^{1}H NMR spectrum of Ac-L-Tyr-2,4-MePro-NHMe. The lower field resonance of each pro-chiral pair is designated with the symbol d, for downfield (i.e., $C^{\beta}H^{exo,d}$, $C^{\beta}H^{endo,d}$, and $C^{\delta}H^{d}$), and the upperfield resonance of each pair with the symbol u, for upfield (i.e., $C^{\beta}H^{exo,u}$, $C^{\beta}H^{endo,u}$, and $C^{\delta}H^{u}$), since absolute pro-chirality[40] assignments (i.e., *pro-R* vs. *pro-S*) were not made.

Peptide bond trans/cis isomerization is slow on the ^{1}H NMR time scale[1-5] at 27 °C and generally gives rise to a separate set of resonances for the cis and trans conformers. Although there is evidence for a small amount (≲5%) of a minor second conformation of Ac-2,4-MePro-NHMe in water (Figure 2A, as discussed below), the data of Figure 2B for Ac-Tyr-2,4-MePro-NHMe indicate that all of the molecules are restricted to one conformational ensemble on the time scale of the ^{1}H NMR experiment. The aromatic proton resonances of tyrosine, which can be used to identify cis/trans heterogeneity in both Tyr-Pro[41-43]

(33) Talluri, S.; Montelione, G. T.; Van Duyne, G.; Piela, L.; Clardy, J.; Scheraga, H. A., in preparation.
(34) Piela, L.; Némethy, G.; Scheraga, H. A., in preparation.
(35) Momany, F. A.; Carruthers, L. M.; McGuire, R. F.; Scheraga, H. A. *J. Phys. Chem.* **1974**, *78*, 1595.
(36) The designations X-Pro and X-(2,4-MePro) refer to dipeptide sequences in which X is the L-α-amino acid preceding proline or 2,4-methanoproline, respectively.
(37) Billeter, M.; Braun, W.; Wüthrich, K. *J. Mol. Biol.* **1982**, *155*, 321.
(38) Karplus, M. *J. Chem. Phys.* **1959**, *30*, 11.
(39) Karplus, M. *J. Am. Chem. Soc.* **1963**, *85*, 2870.
(40) Hanson, K. R. *J. Am. Chem. Soc.* **1966**, *88*, 2731.
(41) Toma, F.; Fermandjian, S.; Low, M.; Kisfaludy, L. *Biochim. Biophys. Acta* **1978**, *534*, 112.

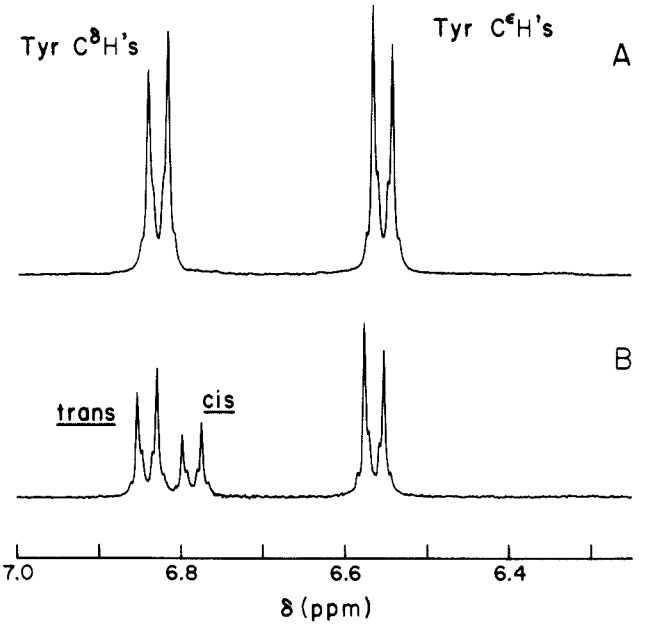

Figure 3. Aromatic ^{1}H NMR resonances of (A) Ac-L-Tyr-2,4-MePro-NHMe and (B) Ac-L-Tyr-L-Pro-NHMe in D_2O at 25 °C. In Ac-L-Tyr-L-Pro-NHMe, the C$^{\delta}$H aromatic resonances of Tyr have different chemical shifts for cis and trans Tyr-Pro peptide bond conformers[41-43] because ensemble-averaged chemical shifts are generally different for slowly interconverting conformational ensembles. The major and minor conformational ensembles of Ac-L-Tyr-L-Pro-NHMe have been assigned to sets of conformers with trans and cis Tyr-Pro peptide bonds, respectively, by NOE spectroscopy (unpublished results). The absence of such chemical shift heterogeneity in Ac-L-Tyr-2,4-MePro-NHMe indicates that one Tyr-2,4-MePro peptide bond conformation predominates in aqueous solution.

Table II. Interproton Coupling within the Methanopyrrolidine Side Chain Observed in the DQF-COSY Spectrum of Ac-2,4-MePro-NHMe[a]

	C$^{\beta}$H^{exo}	C$^{\beta}$H^{endo}	C$^{\gamma}$H	C$^{\delta}$H
C$^{\beta}$H^{exo}	–	×[b]	×	×
C$^{\beta}$H^{endo}	×	–		
C$^{\gamma}$H	×		–	×
C$^{\delta}$H	×		×	–

[a] The C$^{\beta}$H^{exo}, C$^{\beta}$H^{endo}, and C$^{\delta}$H resonances each arise from two degenerate protons. [b] The × designates that a COSY cross-peak was observed in the spectrum shown in Figure 4.

and X-Pro-Tyr[43] sequences, also indicate a single conformational ensemble for Ac-L-Tyr-2,4-MePro-NHMe in water (Figure 3). Similar results were obtained from ^{13}C NMR spectroscopy (data not shown). These ^{1}H and ^{13}C NMR data provide clear evidence that a single X-2,4-MePro peptide bond conformation predominates in these two peptides in aqueous solution.

For Ac-2,4-MePro-NHMe, inspection of the ^{1}H NMR spectrum reveals a second, minor resonance (i.e., the small, unlabeled resonances in Figure 2A) associated with each major resonance. Integration of the proton spectrum reveals that the minor resonances correspond to <5% of the molecules in solution. These minor resonances were shown to correspond to a second molecular

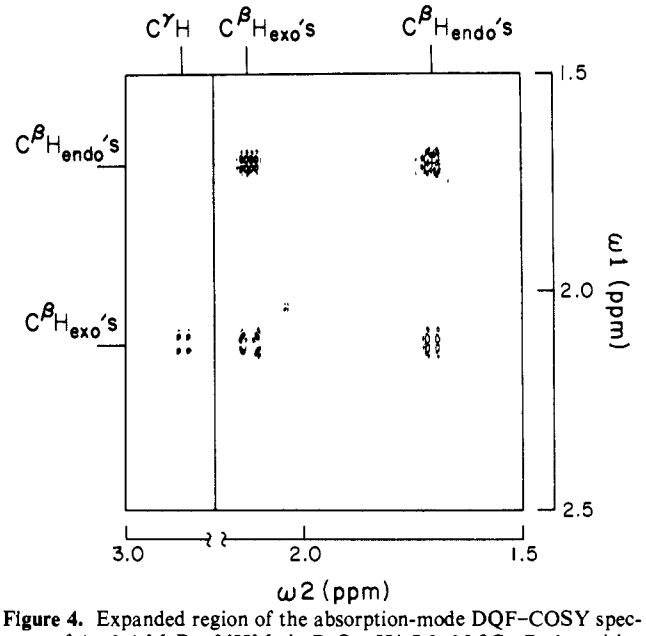

Figure 4. Expanded region of the absorption-mode DQF-COSY spectrum of Ac-2,4-MePro-NHMe in D_2O, pH* 7.0, 25 °C. Both positive and negative contours are plotted.

conformation, rather than to a contaminating peptide, by several different criteria. First, the ratio of minor to major resonances is not altered following repetitive recrystallizations from ethyl acetate, indicating that the minor resonances are not due to a contaminant. Second, the purity of Ac-2,4-MePro-NHMe was established by reversed-phase HPLC (see Methods section). Furthermore, the ratio of the minor to major species is solvent dependent since a larger fraction of the minor species is observed in dimethyl sulfoxide solution (data not shown). The structural difference(s) between this minor (<5%) and the predominant conformational ensembles of Ac-2,4-MePro-NHMe are not yet known (but, see the comments in the Discussion section).

Homonuclear Correlated Spectroscopy (COSY). Double-quantum filtered COSY spectra of Ac-2,4-MePro-NHMe and Ac-L-Tyr-2,4-MePro-NHMe were obtained in D_2O. The interproton couplings identified in these DQF-COSY spectra are summarized in Tables II and III, and expanded regions of the spectra are presented in Figures 4 and 5.

The bicyclic side chain of 2,4-MePro has three pairs of symmetrically positioned protons, viz., C$^{\beta,R}$H^{endo} and C$^{\beta,S}$H^{endo}, C$^{\beta,R}$H^{exo} and C$^{\beta,S}$H^{exo}, and C$^{\delta}$H^{R} and C$^{\delta}$H^{S}. The R and S notation refers to the corresponding prochiralities[40] *pro-R* and *pro-S* of the C$^{\beta}$ atoms with respect to the C$^{\alpha}$ atoms or the C$^{\delta}$H protons with respect to the C$^{\delta}$ atom. This side-chain symmetry is illustrated in Figure 1. For Ac-2,4-MePro-NHMe, the two protons in each of these three pairs are magnetically equivalent, giving rise to a single resonance for each pair of protons. The three resonances arising from these three pairs of degenerate protons (viz. C$^{\beta}$H^{endo}, C$^{\beta}$H^{exo}, and C$^{\delta}$H) are assigned in Figure 2A.

Although much of the intraresidue coupling information is lost because of this degeneracy, some pertinent structural information can still be obtained from the DQF-COSY spectrum of Ac-2,4-MePro-NHMe. In particular, while measurable spin coupling

Table III. Interproton Couplings within the Methanopyrrolidine Side Chain Observed in the DQF-COSY Spectrum of Ac-L-Tyr-2,4-MePro-NHMe

	C$^{\beta}$H^{exo,d}	C$^{\beta}$H^{exo,u}	C$^{\beta}$H^{endo,d}	C$^{\beta}$H^{endo,u}	C$^{\gamma}$H	C$^{\delta}$H^{d}	C$^{\delta}$H^{u}
C$^{\beta}$H^{exo,d}	–		×[a]		×		×
C$^{\beta}$H^{exo,u}		–		×	×	×	
C$^{\beta}$H^{endo,d}	×		–	×			
C$^{\beta}$H^{endo,u}		×	×	–			
C$^{\gamma}$H	×	×			–	×	×
C$^{\delta}$H^{d}		×			×	–	×
C$^{\delta}$H^{u}	×				×	×	–

[a] The × designates that a COSY cross-peak was observed in the spectrum shown in Figure 5.

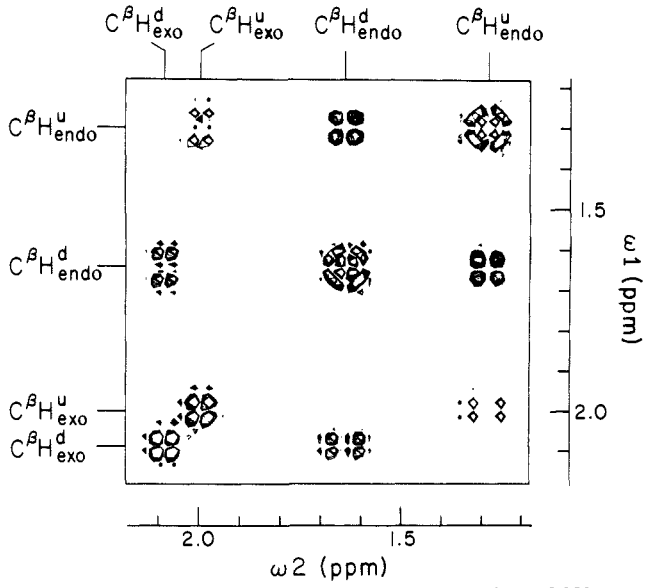

Figure 5. Expanded region of the absorption-mode DQF-COSY spectrum of Ac-L-Tyr-2,4-MePro-NHMe in D_2O, pH* 7.0, 25 °C. Both positive and negative contours are plotted.

is observed between the $C^{\gamma}H$ proton and both the $C^{\delta}H$ and $C^{\beta}H^{exo}$ sets of protons, no coupling is observed between the $C^{\gamma}H$ proton and the two (equivalent) $C^{\beta}H^{endo}$ protons (Figure 4). This result is consistent with the assignments of Figure 2A since (for a symmetric methanopyrrolidine geometry) the calculated $^3J(HC^{\gamma}-C^{\beta}H^{endo})$ vicinal coupling constant (−0.05 Hz) is much smaller than the calculated $^3J(HC^{\gamma}-C^{\beta}H^{exo})$ and $^3J(HC^{\gamma}-C^{\delta}H)$ vicinal coupling constants (3.2 Hz and 1.6 Hz, respectively). Hence, the $C^{\beta}H^{endo}$ and $C^{\beta}H^{exo}$ protons of the 2,4-MePro side chain can be distinguished by their different vicinal couplings to the $C^{\gamma}H$ proton. The absence of a COSY cross-peak between the $C^{\gamma}H$ and $C^{\beta}H^{endo}$ protons and presence of a cross-peak between $C^{\gamma}H$ and $C^{\beta}H^{exo}$ protons in the DQF-COSY spectrum of Ac-2,4-MePro-NHMe (Figure 4) therefore provide verification of the assignments of the $C^{\beta}H^{endo}$ and $C^{\beta}H^{exo}$ resonances.

An additional feature observed in the DQF-COSY spectrum of Ac-2,4-MePro-NHMe is a weak cross-peak between the two $C^{\delta}H$ protons and the two $C^{\beta}H^{exo}$ protons. ^1H NMR data described below for Ac-L-Tyr-2,4-MePro-NHMe indicate that this weak cross-peak arises from long-range couplings $^4J(H^RC^{\delta}-C^{\beta}H^{exo,S})$ and $^4J(H^SC^{\delta}-C^{\beta}H^{exo,R})$. The significance of these long-range couplings is addressed in the Discussion section.

In Ac-L-Tyr-2,4-MePro-NHMe, the magnetic anisotropy arising from the aromatic tyrosine side chain breaks the degeneracy of the $C^{\delta}H$, $C^{\beta}H^{endo}$, and $C^{\beta}H^{exo}$ proton pairs, as can be seen by comparing spectra A and B in Figure 2. This aromatic ring-anisotropy effect on chemical shift (i.e., upfield shift) is stronger for one proton of each of these pairs (designated $C^{\delta}H^{u}$, $C^{\beta}H^{exo,u}$, and $C^{\beta}H^{endo,u}$). Apparently, these three upfield-shifted protons are on the same prochiral face of the 2,4-methanopyrrolidine symmetry plane. This conclusion is consistent with the spin–spin coupling and NOE data described below. The upfield shifts of these protons indicates that, in the ensemble-average, the tyrosine side chain is near one chiral face of the 2,4-MePro side chain. It should be noted that the splitting of the $C^{\delta}H$, $C^{\beta}H^{exo}$, and $C^{\beta}H^{endo}$ resonances (Figure 2B) *cannot* be attributed to two slowly interconverting conformations of Ac-L-Tyr-2,4-MePro-NHMe since spin/spin couplings between $C^{\delta}H^{d}$ and $C^{\delta}H^{u}$ and between $C^{\beta}H^{endo,d}$ and $C^{\beta}H^{endo,u}$ were observed in the DQF-COSY spectrum (Figure 5 and Table III).

The set of interproton couplings identified in the DQF-COSY spectrum (Figure 5, summarized in Table III) of Ac-L-Tyr-2,4-MePro-NHMe is consistent with the assignments shown in Figure 2B. Cross-peaks corresponding to the geminal $^2J(H^{endo,d}C^{\beta}H^{exo,d})$, $^2J(H^{endo,u}C^{\beta}H^{exo,u})$, and $^2J(H^dC^{\delta}H^u)$ and vicinal $^3J(HC^{\gamma}-C^{\beta}H^{exo,d})$, $^3J(HC^{\gamma}-C^{\beta}H^{exo,u})$, $^3J(HC^{\gamma}-C^{\delta}H^d)$, and $^3J(HC^{\gamma}-C^{\delta}H^u)$ couplings are clearly observed. As in Ac-2,4-MePro-NHMe, cross-peaks were not observed for the very weak $^3J(HC^{\gamma}-C^{\beta}H^{endo,d})$ and $^3J(HC^{\gamma}-C^{\beta}H^{endo,u})$ vicinal couplings because these proton dihedral angles are about 80°.

In addition to these geminal and vicinal interproton couplings, longer range couplings within the 2,4-methanopyrrolidine side chain were also observed. Of particular interest is the strong COSY cross-peak between the $C^{\beta}H^{endo,d}$ and $C^{\beta}H^{endo,u}$ protons (Figure 5) (J = 10.0 Hz) which indicates a significant electronic interaction between $C^{\beta,R}H_2$ and $C^{\beta,S}H_2$ methylene groups. Furthermore, the couplings between (two equivalent) $C^{\delta}H$ and the (two equivalent) $C^{\beta}H^{exo}$ protons observed for Ac-2,4-MePro-NHMe are resolved in Ac-L-Tyr-2,4-MePro-NHMe into distinct $C^{\delta}H^d/C^{\beta}H^{exo,u}$ and $C^{\delta}H^u/C^{\beta}H^{exo,d}$ cross-peaks (Figure 5; Table III). The significance of these weak long-range couplings is addressed in the Discussion section.

Distinguishing between Cis and Trans Peptide Bond Conformations by Considerations of Distance Geometry. From the one- and two-dimensional ^1H NMR data described above, we conclude that a single X-2,4-MePro peptide bond conformation predominates (i.e., ≳95%) for Ac-2,4-MePro-NHMe and Ac-L-Tyr-2,4-MePro-NHMe in aqueous solution at 25 °C. Here, we describe how interproton distance information was used to determine whether this peptide bond conformation is cis or trans. A similar approach has recently been suggested for distinguishing between cis and trans X-proline peptide bonds.[44,45]

In the dipeptide fragment X-2,4-MePro, where X is an α-amino acid cis and trans peptide bond conformations can be distinguished even by *qualitative* measurements of the X—$C^{\alpha}H$···2,4-MePro—$C^{\delta}H$ interproton distances, which depend on both the peptide bond conformation (dihedral angle ω_X) and the backbone dihedral angle ψ_X of residue X. For a planar trans X-2,4-MePro peptide bond conformation (with the symmetrized geometry tabulated in Table I, and the L configuration of amino acid X), the ψ_X interproton distances are

$$d^{trans}_{\alpha,\delta R} = |(10.46 + 5.58 \cos\theta + 1.80 \sin\theta)^{1/2}| \quad (2)$$

and

$$d^{trans}_{\alpha,\delta S} = |(10.46 + 5.58 \cos\theta - 1.80 \sin\theta)^{1/2}| \quad (3)$$

where $d^{trans}_{\alpha,\delta R}$ and $d^{trans}_{\alpha,\delta S}$ are the interproton distances for the *pro-R* and *pro-S* 2,4-MePro $C^{\delta}H$ protons, respectively, and $\theta = \psi_X + 60°$. For a planar cis X-2,4-MePro peptide bond conformation (with the symmetrized geometry tabulated in Table I and the L configuration for amino acid X) the corresponding equations are

$$d^{cis}_{\alpha,\delta R} = |(22.79 + 2.32 \cos\theta - 1.80 \sin\theta)^{1/2}| \quad (4)$$

and

$$d^{cis}_{\alpha,\delta S} = |(22.79 + 2.32 \cos\theta + 1.80 \sin\theta)^{1/2}| \quad (5)$$

In Figure 6, we present plots of the Tyr $C^{\alpha}H$···2,4-MePro $C^{\delta}H^R$ and Tyr $C^{\alpha}H$···2,4-MePro $C^{\delta}H^S$ interproton distances as a function of ψ_{Tyr} for trans and cis L-Tyr-2,4-MePro peptide bond conformations. For a trans peptide bond, these internuclear distances range from 2.1 to 4.0 Å, depending on the value of ψ_{Tyr}, while for a cis peptide bond, the internuclear distances range from 4.5 to 5.1 Å. Similar results are obtained for the acetyl methyl proton/$C^{\delta}H$ proton internuclear distances of Ac-2,4-MePro-NHMe. These ranges of interproton distances are approximately the same for all X-2,4-MePro peptide fragments, when X is an L-α-amino acid. Because these ranges of $C^{\alpha}H/C^{\delta}H$ interproton distances which characterize X-2,4-MePro trans and cis peptide

(42) Toma, F.; Fermandjian, S.; Low, M.; Kisfaludy, L. *Biopolymers* **1981**, *20*, 901.
(43) Stimson, E. R.; Montelione, G. T.; Meinwald, Y. C.; Rudolph, R. K. E.; Scheraga, H. A. *Biochemistry* **1982**, *21*, 5252.
(44) Arseniev, A. S.; Kondakov, V. I.; Maiorov, V. N.; Volkava, T. M.; Grishen, E. V.; Bystrov, V. F.; Ovchinnikov, Yu. A. *Bioorgan. Khim.* **1983**, *9*, 768.
(45) Wüthrich, K.; Billeter, M.; Braun, W. *J. Mol. Biol.* **1984**, *180*, 715.

Table IV. Distance Matrix (Å) for Protons of the Methanopyrrolidine Side Chain of 2,4-MePro Determined from the Crystal Structure[a]

	$C^{\beta,R}H^{exo}$	$C^{\beta,S}H^{exo}$	$C^{\beta,R}H^{endo}$	$C^{\beta,S}H^{endo}$	$C^{\gamma}H$	$C^{\delta}H^{R}$	$C^{\delta}H^{S}$
$C^{\beta,R}H^{exo}$	–	2.58	1.75	3.67	2.77	3.78	4.34
$C^{\beta,S}H^{exo}$		–	3.67	1.75	2.77	4.34	3.78
$C^{\beta,R}H^{endo}$			–	4.04	2.91	2.56	3.69
$C^{\beta,S}H^{endo}$				–	2.91	3.69	2.56
$C^{\gamma}H$					–	2.59	2.59
$C^{\delta}H^{R}$						–	1.75
$C^{\delta}H^{S}$							–

[a] The heavy atoms of the Ac-2,4-MePro-NHMe crystal structure[33] were symmetrized[34] and the protons added with ideal bond lengths and bond angles, as described in the Methods section.

Table V. Fractional Increases in Areas of Proton Resonances Observed in Steady-State Measurements of Truncated Overhauser Effects within the 2,4-Methanopyrrolidine Side Chain of Ac-L-Tyr-2,4-MePro-NHMe

proton irradiated ↓	$C^{\beta}H^{exo,d}$	$C^{\beta}H^{exo,u}$	$C^{\beta}H^{endo,d}$	$C^{\beta}H^{endo,u}$	$C^{\gamma}H$	$C^{\delta}H^{d}$	$C^{\delta}H^{u}$
$C^{\beta}H^{exo,d}$	–	*a*	0.29 ± 0.02	N.O.[c]	0.08 ± 0.01	N.O.	N.O.
$C^{\beta}H^{exo,u}$	*a*, *b*	–	*b*	*b*	*b*	*b*	*b*
$C^{\beta}H^{endo,d}$	0.31 ± 0.05	N.O.	–	*a*	N.O.	0.05 ± 0.01	N.O.
$C^{\beta}H^{endo,u}$	N.O.	0.30 ± 0.03	*a*	–	N.O.	N.O.	0.04 ± 0.02
$C^{\gamma}H$	0.02 ± 0.01	0.03 ± 0.01	N.O.	N.O.	–	0.03 ± 0.01	0.03 ± 0.01
$C^{\delta}H^{d}$	N.O.	N.O.	0.04 ± 0.02	N.O.	0.08 ± 0.01	–	0.30 ± 0.02
$C^{\delta}H^{u}$	N.O.	N.O.	N.O.	0.05 ± 0.01	0.08 ± 0.01	0.23 ± 0.01	–

[a] Any interproton NOE which may be present could not be measured reliably by the difference truncated Overhauser method because the difference in chemical shift between these resonances is small. [b] Proton Overhauser effects resulting from irradiation of the $C^{\beta}H^{exo,u}$ proton could not be identified reliably because the $C^{\beta}H^{exo,u}$ and acetyl CH_3 proton resonances are overlapped. [c] Not observed.

bond conformations are different and not overlapping, they can be distinguished by relatively imprecise estimates of interproton distances obtained from measurements of nuclear Overhauser effects.

Calibration of Interproton Overhauser Effects. From the distance–geometry arguments presented in the previous section and in Figure 6 it is evident that, for a unique backbone conformation, precise measurements of the two $C^{\alpha}H/C^{\delta}H$ interproton distances across an X-2,4-MePro peptide bond can be used to determine not only the intervening peptide bond conformation but also the backbone dihedral angle ψ of the residue X preceding 2,4-MePro. In Ac-L-Tyr-2,4-MePro-NHMe, however, ψ_{Tyr} probably adopts several values. Furthermore, a precise calculation of this interproton distance from proton Overhauser measurements requires proper modeling of the relative internuclear motions between these protons. Since no information is presently available about the molecular dynamics of these molecules in solution, no attempt was made to calculate precise interproton distances. Instead, the interproton NOEs between the seven protons of the methanopyrrolidine side chain of 2,4-MePro are used to determine an empirical upper bound for interproton distances which are sufficiently short to be observed in our NOE measurements. The calibration was then used to determine whether the conformationally averaged Tyr $C^{\alpha}H/2,4$-MePro $C^{\delta}H$ interproton distances are characteristic of a trans (i.e., <4.0 Å) or cis (i.e., >4.5 Å) peptide bond conformation.

There are 21 distinguishable interproton distances (i.e., $N(N-1)/2$ distinguishable interpoint distances between N points) between the seven methanopyrrolidine side-chain protons of 2,4-MePro. These 21 distances, calculated from the symmetrized crystal structure of Ac-2,4-MePro-NHMe (see Methods section), are presented in the form of a (symmetric) distance matrix in Table IV. These fixed interproton distances range from 1.75 to 4.34 Å.

In Table V, we present the results of steady-state truncated interproton Overhauser measurements between the seven methanopyrrolidine side-chain protons of Ac-L-Tyr-2,4-MePro-NHMe. It should be noted that, in these one-dimensional NOE measurements, we cannot obtain reliable information from irradiation of the 2,4-MePro $C^{\beta}H^{exo,u}$ resonance since its chemical shift is very similar to that of the acetyl methyl protons (Figure 2B). Comparison of Tables IV and V reveals that, under the conditions of these NOE measurements, no Overhauser effects are observed between methanopyrrolidine protons greater than 2.6 Å apart, the approximate cutoff lying between 2.6 and 2.9 Å. In particular,

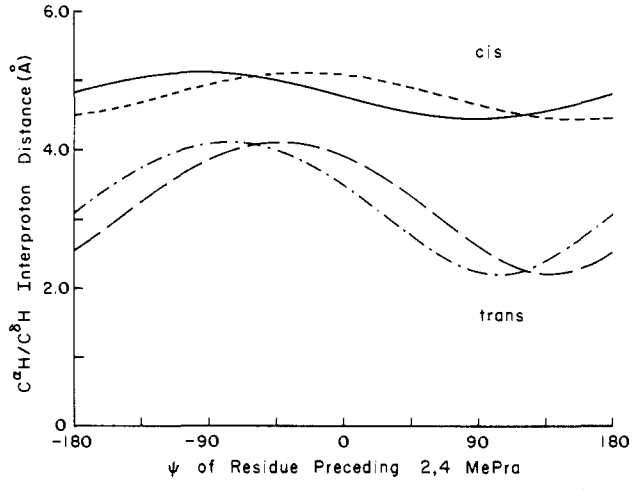

Figure 6. Conformation dependence of Tyr $C^{\alpha}H/2,4$-MePro $C^{\delta}H$ interproton distances for cis and trans Tyr-2,4-MePro peptide bond conformations ($\omega = 0°$ and 180°, respectively). (-·-) Tyr $C^{\alpha}H/2,4$-MePro $C^{\delta}H^{S}$ interproton distance for trans Tyr-2,4-MePro peptide bond. (---) Tyr $C^{\alpha}H/2,4$-MePro $C^{\delta}H^{R}$ interproton distance for trans Tyr-2,4-MePro peptide bond. (—) Tyr $C^{\alpha}H/2,4$-MePro $C^{\delta}H^{R}$ interproton distance for cis Tyr-2,4-MePro peptide bond. (---) Tyr-$C^{\alpha}H/2,4$-MePro $C^{\delta}H^{S}$ interproton distance for cis Tyr-2,4-MePro peptide bond.

there was no evidence for spin-diffusion effects within the 2,4-methanoproline side chain under the conditions of these measurements (Table V). Since relative interproton motion for internuclear distances which are not fixed by bicyclic geometry will tend to attenuate the Overhauser effects, we conclude from these calibration data that NOEs are not observable (i.e., $\eta < 0.002$) under these conditions for (conformationally averaged) interproton distances in Ac-L-Tyr-2,4-MePro-NHMe $\gtrsim$3.0 Å.

Determination of the Predominant Peptide Bond Conformation of Ac-2,4-MePro-NHMe and Ac-L-Tyr-2,4-MePro-NHMe by Measurements of Steady-State Truncated Overhauser Effects. A difference spectrum showing the positive steady-state truncated NOEs for Ac-2,4-MePro-NHMe which results from selective irradiation of the two $C^{\delta}H$ protons is shown in Figure 7. Positive NOEs are observed to the $C^{\gamma}H$ ($d = 2.6$ Å; $\eta = 0.017 \pm 0.002$) and $C^{\beta}H^{endo}$ ($d = 2.6$ and 3.7 Å; $\eta = 0.011 \pm 0.002$) protons, but not to the $C^{\beta}H^{exo}$ protons ($d = 3.8$ and 4.3 Å). As in Ac-L-Tyr-2,4-MePro-NHMe, under the conditions of our measurements

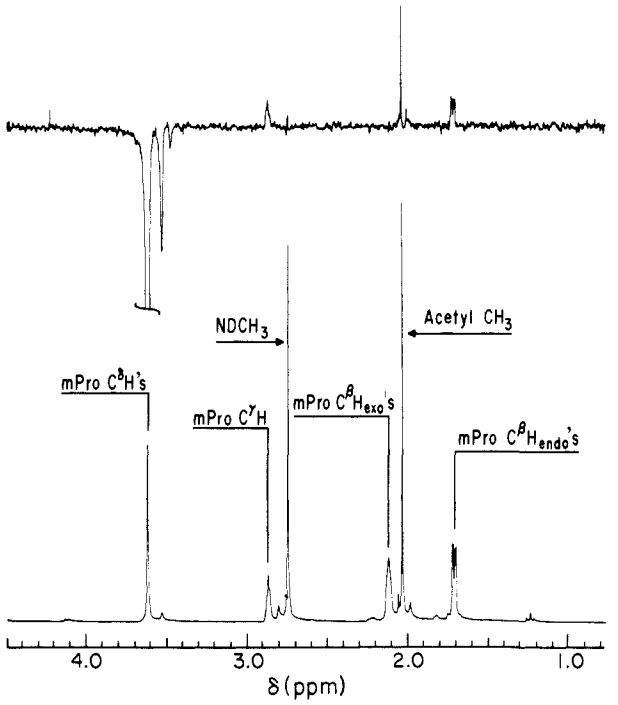

Figure 7. Steady-state truncated driven NOE difference spectrum (top) of Ac-2,4-MePro-NHMe in D_2O with selective irradiation of the (two) 2,4-MePro $C^{\delta}H$ protons. The positive NOE to the acetyl methyl group indicates that the Ac-2,4-MePro peptide bond is trans. The bottom spectrum is a standard one-dimensional ^1H NMR spectrum recorded under the same conditions.

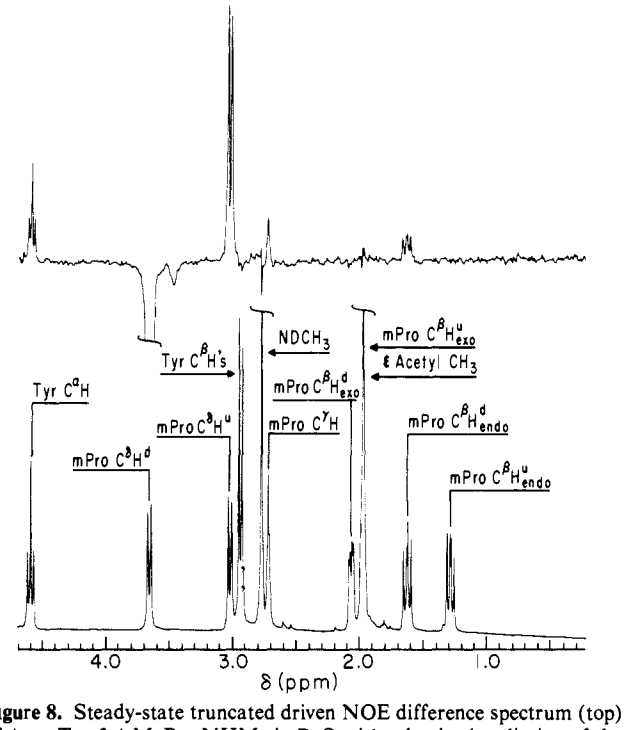

Figure 8. Steady-state truncated driven NOE difference spectrum (top) of Ac-L-Tyr-2,4-MePro-NHMe in D_2O with selective irradiation of the 2,4-MePro $C^{\delta}H^{d}$ resonance. The positive NOE to the Tyr $C^{\alpha}H$ proton indicates that the Tyr-2,4-MePro peptide bond is trans. It should be noted that, in the upper difference spectrum, the small negative peak at ca. 3.5 ppm corresponds to a small amount of a chemical decomposition product which appears over a period of several days in neutral aqueous solution. This decomposition product can be removed by repurification on reversed phase HPLC. The bottom spectrum is a standard one-dimensional ^1H NMR spectrum recorded under the same conditions.

interproton NOEs are not observed for interproton distances >3.0 Å in Ac-2,4-MePro-NHMe.

In addition to these NOE's between protons whose internuclear distances are fixed by the geometry of the methanopyrrolidine side chain, the conformation-dependent NOE between the two $C^{\delta}H$ protons and the acetyl methyl protons ($\eta = 0.007 \pm 0.002$) is also observed in the difference spectra of Figure 7. The presence of this NOE indicates that the corresponding conformationally averaged interproton distance is $\lesssim$3.0 Å. As can be seen from Figure 6, this can be true only if the intervening peptide bond has a trans conformation.

Similar calibrated steady-state NOE measurements were used to determine the unique peptide bond conformation of Ac-L-Tyr-2,4-MePro-NHMe. A second difference spectrum showing the positive steady-state truncated NOEs for Ac-L-Tyr-2,4-MePro-NHMe which result from selective irradiation of the $C^{\delta}H^{d}$ proton of 2,4-MePro is presented in Figure 8. In this difference spectrum (top of Figure 8), positive steady-state NOEs are observed to the $C^{\delta}H^{u}$ ($d = 1.8$ Å; $\eta = 0.30 \pm 0.02$), $C^{\gamma}H$ ($d = 2.6$ Å; $\eta = 0.08 \pm 0.01$), and $C^{\beta}H^{endo,d}$ ($d = 2.6$ Å; $\eta = 0.04 \pm 0.01$) protons of the methanopyrrolidine side chain, but not to the $C^{\beta}H^{endo,u}$ ($d = 3.7$ Å), $C^{\beta}H^{exo,d}$ ($d = 3.8$ Å), and $C^{\beta}H^{exo,u}$ ($d = 4.3$ Å) protons. Since NOEs are not observed in Ac-L-Tyr-2,4-MePro-NHMe under the conditions of our measurements for internuclear distances greater than 3.0 Å, we can safely conclude that $C^{\alpha}H/C^{\delta}H$ NOEs will be observed only if the intervening peptide bond is trans.

The strong positive 2,4-MePro $C^{\delta}H^{d}$/Tyr $C^{\alpha}H$ NOE ($\eta = 0.12 \pm 0.02$) is shown in the top of Figure 8. In addition, the 2,4-MePro $C^{\delta}H^{u}$/Tyr $C^{\alpha}H$ ($\eta = 0.06 \pm 0.01$), Tyr $C^{\alpha}H$/2,4-MePro $C^{\delta}H^{d}$ ($\eta = 0.06 \pm 0.01$), and Tyr $C^{\alpha}H$/2,4-MePro $C^{\delta}H^{u}$ ($\eta = 0.04 \pm 0.01$) steady-state NOEs were also observed in separate truncated difference NOE spectra (not shown here). This set of Tyr $C^{\alpha}H$/2,4-MePro $C^{\delta}H$ NOEs demonstrates that these two (conformationally averaged) interproton distances are <3.0 Å. This can be true only if the intervening Tyr-2,4-MePro peptide bond is trans.

Simultaneous Calibration of Interproton Overhauser Effects and Determination of Predominant Peptide Bond Conformation of Ac-L-Tyr-2,4-MePro-NHMe by Absorption Mode NOESY. In the previous two sections, we described how a series of steady-state truncated Overhauser effect measurements were used to determine the predominant X-2,4-MePro peptide bond conformations of Ac-2,4-MePro-NHMe and Ac-L-Tyr-2,4-MePro-NHMe in water. This same information can be obtained from a single absorption mode NOESY spectrum. The absorption mode NOESY spectrum of Ac-L-Tyr-2,4-MePro-NHMe was obtained, and quantitative estimates of relative cross-peak intensities between protons of the 2,4-methanopyrrolidine side chain are presented in Table VI. Comparison of Table VI with the distance matrix of Table IV demonstrates that, under the conditions of these two-dimensional NMR measurements, no NOESY cross-peaks are observed between protons separated by more than 3.0 Å. As in the one-dimensional experiments, there was no evidence for intramolecular spin-diffusion effects (Table VI). Hence, on the basis of the calculations shown in Figure 6, we would anticipate Tyr $C^{\alpha}H$/2,4-MePro $C^{\delta}H$ NOESY cross-peaks only if the intervening peptide bond is in the trans conformation. These cross-peaks are clearly seen in cross sections of the NOESY spectrum shown in Figure 9. Quantitative estimates of these cross-peak intensities are presented in Table VII.

Determination of ψ_{Tyr} in *trans*-Ac-Tyr-2,4-MePro-NHMe from Distance Constraints. The distance constraints determined above indicate that *both* (ensemble-averaged) Tyr $C^{\alpha}H$···2,4-MePro $C^{\delta}H^{d}$ and Tyr $C^{\alpha}H$···2,4-MePro $C^{\delta}H^{u}$ interproton distances are <3.0 Å. Hence, according to Figure 6, the observed NOEs arise from conformation(s) in which $70° < \psi_{Tyr} < 170°$; i.e., a significant fraction of trans Ac-L-Tyr-2,4-MePro-NHMe molecules has ψ_{Tyr} in this range. These measurements, however, do not rule out a population of conformers with ψ_{Tyr} outside this range which do not contribute to the observed nuclear Overhauser effect.

Discussion

Selective Stabilization of Trans Peptide Bonds of 2,4-MePro. The NMR results presented here demonstrate that for both

Table VI. Ratios of Cross-Peak/Diagonal-Peak Areas for Dipolar Couplings within the Methanopyrrolidine Side Chain Obtained from the Phase Sensitive NOESY Spectrum of Ac-L-Tyr-2,4-MePro-NHMe[a]

	$C^{\beta}H^{exo,d}$	$C^{\beta}H^{exo,u}$	$C^{\beta}H^{endo,d}$	$C^{\beta}H^{endo,u}$	$C^{\gamma}H$	$C^{\delta}H^{d}$	$C^{\delta}H^{u}$
$C^{\beta}H^{exo,d}$	–	N.O.[b]	0.206 ± 0.014[c]	N.O.	0.018 ± 0.010	N.O.	N.O.
$C^{\beta}H^{exo,u}$	N.O.	–	N.O.	0.200 ± 0.013	0.024 ± 0.007	N.O.	N.O.
$C^{\beta}H^{endo,d}$	0.203 ± 0.012	N.O.	–	N.O.	N.O.	0.022 ± 0.011	N.O.
$C^{\beta}H^{endo,u}$	N.O.	0.155[d]	N.O.	–	N.O.	N.O.	0.015 ± 0.006
$C^{\gamma}H$	N.O.	N.O.	0.017 ± 0.005	0.012 ± 0.003	–	0.010 ± 0.005	N.O.
$C^{\delta}H^{d}$	N.O.	N.O.	0.033 ± 0.007	N.O.	0.017 ± 0.003	–	0.192 ± 0.011
$C^{\delta}H^{u}$	N.O.	N.O.	N.O.	0.039 ± 0.003	0.019 ± 0.004	0.165 ± 0.003	–

[a] Data are derived from cross sections of a NOESY spectrum which was obtained with an optimized mixing time of 350 ms. [b] Not observed. [c] Error estimates reflect the ranges of values obtained by integrating several $\omega 1$ cross sections. [d] This cross-peak intensity could not be computed accurately because of interference from a t_1-noise artifact of the acetyl methyl resonance, which was not completely suppressed by the double quantum filter.

Table VII. Ratios of Cross-Peak/Diagonal-Peak Areas for Conformation-Dependent NOEs in Ac-L-Tyr-2,4-MePro-NHMe[a]

	TyrC$^{\alpha}$H	mProC$^{\delta}$H^{d}	mProC$^{\delta}$H^{u}
TyrC$^{\alpha}$H	–	0.036 ± 0.004[b]	0.014 ± 0.003
mProC$^{\delta}$H^{d}	0.042 ± 0.001	–	0.192[c] ± 0.011
mProC$^{\delta}$H^{u}	0.031 ± 0.001	0.165[c] ± 0.003	–

[a] Data are derived from cross sections of the NOESY spectrum shown in Figure 9, which was obtained with a mixing time of 350 ms. [b] Error estimates reflect the ranges of values obtained by integrating several $\omega 1$ cross sections. [c] Conformation-independent methylene cross-peaks.

Ac-2,4-MePro-NHMe and Ac-L-Tyr-2,4-MePro-NHMe the trans X-2,4-MePro peptide bond conformers are selectively stabilized in aqueous solution. These results are consistent with the X-ray crystal structure[33] and with conformational energy calculations[34] of Ac-2,4-MePro-NHMe, in which the Ac-2,4-MePro peptide is also trans. It should be noted that the initial interpretation of these NMR data used geometry derived from the X-ray structure[17] of the free amino acid 2,4-MePro for which the bond lengths and bond angles of the Ac-2,4-MePro peptide group were approximated. In this way, the NMR data were used to determine the peptide bond conformation before the crystal structure of Ac-2,4-MePro-NHMe was determined. Subsequently, the coefficients of eq 2–5 and the distances in Table IV were recalculated with use of parameters derived from the crystal structure of Ac-2,4-MePro-NHMe.

The cis/trans X-Pro peptide bond equilibrium constants for Ac-L-Pro-NHMe[15] ($K_{t\rightarrow c}$ = 0.33) and Ac-L-Tyr-L-Pro-NHMe[43] ($K_{t\rightarrow c}$ = 0.54) in neutral D_2O solution at 25 °C have been reported elsewhere. Introduction of a methylene bridge between the α and γ carbons of L-proline in either of these peptides results in a selective stabilization of the trans peptide bond conformation in water ($K_{t\rightarrow c} \leq 0.05$). An examination of intramolecular interactions in models of cis and trans Ac-L-Tyr-2,4-MePro-NHMe suggests that the preferential stabilization of the trans conformation arises from unfavorable steric interactions between the atoms of the peptide group following 2,4-MePro (i.e., the 2,4-MePro-NHMe peptide group) and the tyrosine backbone (C^{α}HNH) and side chain atoms in cis X-2,4-MePro peptide bond conformers. These interactions are much more unfavorable for cis Ac-L-Tyr-2,4-MePro-NHMe than for cis Ac-L-Tyr-L-Pro-NHMe since the backbone dihedral angle ϕ of 2,4-methanoproline is restricted to values near 0° by its bicyclic side-chain structure, while in L-proline, ϕ is conformationally restricted to values[31] of −68° to −75°. In Ac-2,4-MePro-NHMe, similar unfavorable interactions between atoms of the 2,4-MePro-NHMe peptide group and the acetyl methyl group in the cis X-2,4-MePro peptide bond conformation appear to be the principal cause of the selective stabilization of the trans conformer. It should be noted, however, that a small amount of a second Ac-2,4-MePro-NHMe conformer is detected in aqueous solution. This may possibly correspond to a small population of energetically accessible cis Ac-2,4-MePro-NHMe conformers. This suggests that the unfavorable interactions which destabilize cis Ac-L-Tyr-2,4-MePro-NHMe are partially relieved when the Ac-Tyr group is replaced with a less bulky acetyl group. A more detailed conformational analysis,

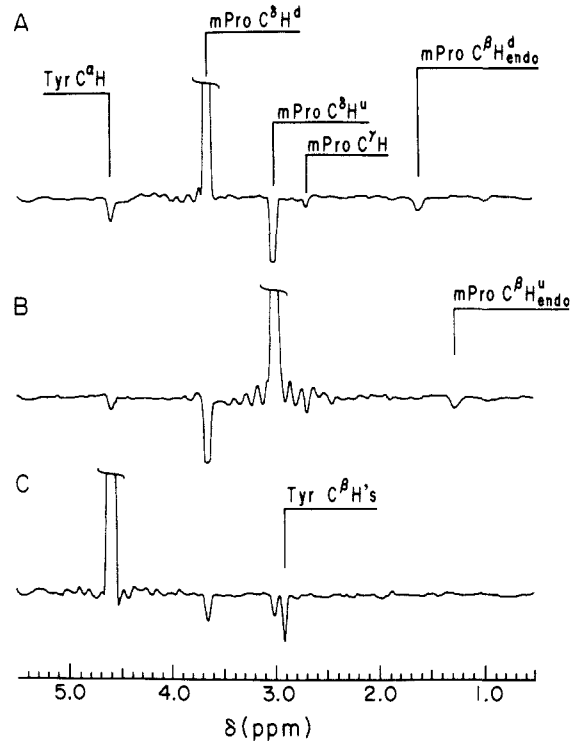

Figure 9. $\omega 1$ cross sections from absorption-mode NOESY spectrum of Ac-L-Tyr-2,4-MePro-NHMe in D_2O, pH* 7.0, 25 °C, obtained with a mixing time of 350 ms. In this spectrum, the diagonal peaks are positive and the cross-peaks are negative. No artificial symmetrization routines were used. (A) $\omega 1$ cross section through 2,4-MePro $C^{\delta}H^{d}$ proton resonance. (B) $\omega 1$ cross section through 2,4-MePro $C^{\delta}H^{u}$ proton resonance. (C) $\omega 1$ cross section through Tyr $C^{\alpha}H$ proton resonance.

based on conformational energy calculations,[32,35] will be presented elsewhere.[34]

Long-Range Couplings in 2,4-MePro. In the DQF–COSY spectrum of trans Ac-2,4-MePro-NHMe, cross-peaks were observed indicating that there is J coupling between the (two) $C^{\delta}H$ protons and the (two) $C^{\beta}H^{exo}$ protons. In trans Ac-L-Tyr-2,4-MePro-NHMe, these internuclear couplings were identified as two long-range couplings (viz., $C^{\delta}H^{d}/C^{\beta}H^{exo,u}$ and $C^{\delta}H^{u}/C^{\beta}H^{exo,d}$). In addition, a very strong long-range coupling is observed between the $C^{\beta}H^{endo,d}$ and $C^{\beta}H^{endo,u}$ protons of the 2,4-methanopyrrolidine ring of Ac-L-Tyr-2,4-MePro-NHMe. These results indicate significant electronic interactions between the $C^{\delta}H_2$, the *pro-R* $C^{\beta}H_2$, and the *pro-S* $C^{\beta}H_2$ methylene groups of the 2,4-methanopyrrolidine ring. In a subsequent study,[33] we shall demonstrate how these long-range spin/spin coupling constants can be used to detect 2,4-methanopyrrolidine asymmetry in solution.

Acknowledgment. This work was supported by research grants from the National Institute of General Medical Sciences, the National Institutes of Health (GM-24893), and the National Science Foundation (DMB84-01811). We also acknowledge the support of the NIH Nuclear Magnetic Resonance Facility at

Syracuse, New York. We thank S. Rumsey for aid with the molecular graphics and Y. C. Meinwald, G. Némethy, L. Piela, and S. Talluri for helpful discussions.

Registry No. 2,4-MePro-OBzl·TsOH, 103794-05-4; Ac-2,4-MePro-NHMe, 103794-02-1; Ac-2,4-MePro-OBzl, 103794-06-5; Ac-L-Tyr-2,4-MePro-NHMe, 103794-03-2; 2,4-MePro-NHMe, 103794-07-6; Boc-L-Tyr, 3978-80-1; Boc-L-Tyr-2,4-MePro-NHMe, 103794-08-7; L-Tyr-2,4-MePro-NHMe, 103794-09-8; 2,4-methanoproline, 73550-56-8; methylamine, 74-89-5.

Evidence for Conformational Equilibrium of the Sulfated L-Iduronate Residue in Heparin and in Synthetic Heparin Mono- and Oligosaccharides: NMR and Force-Field Studies

Dino R. Ferro,*† Augusto Provasoli,† Massimo Ragazzi,† Giangiacomo Torri,‡ Benito Casu,‡ Giuseppe Gatti,§ Jean-Claude Jacquinet,⊥ Pierre Sinaÿ,⊥ Maurice Petitou,‖ and Jean Choay‖

Contribution from the Istituto di Chimica delle Macromolecole del CNR, via E. Bassini 15/A, I-20133 Milano, Italy, Istituto di Chimica e Biochimica "G. Ronzoni", Milano, Italy, Bruker Spectrospin Italiana, Milano, Italy, Université d' Orléans, France, and Institut Choay, Paris, France. *Received February 13, 1986*

Abstract: The conformation of sulfated L-iduronic acid (I_{2S}) in different heparin sequences, including the specific pentasaccharide sequence representing the binding site to antithrombin III (AT-III), was investigated by ^1H NMR spectroscopy on suitable synthetic mono- and oligosaccharides. For the monomer methyl 2-*O*-sulfo-α-L-iduronate vicinal interproton coupling constants are all small (1.8–3.4 Hz), accounting for a predominant contribution of a $^1C_4$ chair. By contrast, some couplings (especially $J_{2,3}$) become larger (up to 6 Hz) when I_{2S} is inserted between two N,6-disulfated D-glucosamine residues as occurring in the regular sequences of heparin, and even larger (up to 7.5 Hz) when I_{2S} is glycosylated by the *N*,3,6-trisulfated D-glucosamine residue typical of the binding site to AT-III. The interproton coupling constants of the individual, nearly isoenergetic conformers of I_{2S} ($^1C_4$, $^2S_0$, and $^4C_1$) were evaluated for different heparin sequences by using molecular geometries obtained by a force field method. Other conformations were discarded on the basis of energy considerations. The conformer populations were obtained by least-squares fitting the average computed coupling constants of the conformer mixture to the observed values. When I_{2S} is part of regular heparin sequences, the skew-boat form $^2S_0$ becomes an important contributor (~40%) to the conformation of the sulfated iduronate residues. When the amino sugar residue glycosylating the I_{2S} is trisulfated (as in the binding site to AT-III), $^2S_0$ becomes predominant (>60%). Force field calculations suggest that such a drive toward the $^2S_0$ conformation is associated with electrostatic effects of the unique 3-sulfate group.

Heparin, a sulfated polysaccharide belonging to the class of glycosaminoglycans, widely distributed in animal tissues, is currently used in therapy as an anticoagulant and antithrombotic.[1] Heparin acts mainly by binding to antithrombin III (AT-III) and enhancing the inhibitory effect of this protein on a number of procoagulant proteases.[2,3] Other biological activities of heparin are associated with less specific but strong interactions with plasma proteins.[4]

The structure of heparin is largely accounted for by regular sequences of the trisulfated disaccharide **1** {(1→4)-*O*-(2-*O*-sulfo-α-L-idopyranosyluronic acid)-(1→4)-*O*-(2-deoxy-2-sulfamido-6-*O*-sulfo-α-D-glucopyranose)}. However, heparin also contains irregular sequences, including a unique one, the hexasaccharide **2** {*O*-(α-L-idopyranosyluronic acid)-(1→4)-*O*-(2-acetamido-2-deoxy [*or* 2-deoxy-2-sulfamido]-6-*O*-sulfo-α-D-glucopyranosyl)-(1→4)-*O*-(β-D-glucopyranosyluronic acid)-(1→4)-*O*-(2-deoxy-2-sulfamido-3,6-di-*O*-sulfo-α-D-glucopyranosyl-(1→4)-*O*-(2-*O*-sulfo-α-L-idopyranosyluronic acid)-(1→4)-*O*-(2-deoxy-2-sulfoamido-6-*O*-sulfo-α-D-glucopyranose)}.[5-8] Sequence **2** contains the structure responsible for binding to AT-III, i.e., the pentasaccharide sequence $A_{NA/NS,6S}$-G-$A^*_{NS,3,6S}$-I_{2S}-$A_{NS,6S}$ (between dashed lines in formula **2**).[9-14] Among the sulfate groups

Chart I

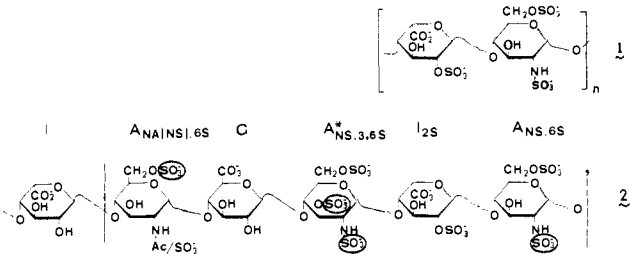

essential for binding to AT-III (encircled in formula **2**),[11] the unique 3-*O*-sulfo group of residue $A^*_{NS,3,6S}$ plays a critical role

* To whom correspondence should be addressed.
† Istituto di Chimica delle Macromolecole del CNR.
‡ Istituto di Chimica e Biochimica "G. Ronzoni".
§ Bruker Spectrospin Italiana.
⊥ Université d' Orléans.
‖ Institut Choay.

(1) Jacques, L. B. *Pharmacol. Rev.* **1980**, *31*, 99–166.
(2) Rosenberg, R. D.; Damus, P. S. *J. Biol. Chem.* **1973**, *248*, 6490–6505.
(3) Björk, I.; Lindahl, U. *Mol. Cell. Biochem.* **1982**, *48*, 161–182.
(4) Casu, B. *Adv. Carbohydr. Chem. Biochem.* **1985**, *43*, 51–134.
(5) Lindahl, U.; Bäckström, G.; Thunberg, L.; Leder, I. G. *Proc. Natl. Acad. Sci. U.S.A.* **1980**, *77*, 6551–6555.
(6) Choay, J.; Lormeau, J.-C.; Petitou, M.; Sinaÿ, P.; Casu, B.; Oreste, P.; Torri, G.; Gatti, G. *Thromb. Res.* **1980**, *18*, 573–578.
(7) Casu, B.; Oreste, P.; Torri, G.; Zoppetti, G.; Choay, J.; Lormeau, J.-C.; Petitou, M.; Sinaÿ, P. *Biochem. J.* **1981**, *197*, 599–609.
(8) Meyer, B.; Thunberg, U.; Lindahl, U.; Larm, O.; Leder, I. G. *Carbohydr. Res.* **1981**, *88*, C1–C4.
(9) Abbreviations used: I = α-L-iduronic acid; G = β-D-glucuronic acid; I_{2S} = 2-sulfate-α-L-iduronate; $A_{NA,6S}$ = *N*-acetyl-α-D-glucosamine 6-sulfate; $A_{NS,6S}$ = α-D-glucosamine *N*,6-disulfate; $A^*_{NS,3,6S}$ = α-D-glucosamine *N*,3,6-trisulfate; AT-III = antithrombin III.

0002-7863/86/1508-6773$01.50/0